

## Dimensional Crossover of Shubnikov-de Haas Oscillations in Thin Films of Gray Tin

S. N. Song, X. J. Yi, J. Q. Zheng, Z. Zhao, L. W. Tu, G. K. Wong, and J. B. Ketterson

*Department of Physics and Astronomy, Northwestern University, and Materials Research Center, Evanston, Illinois 60208*

(Received 27 March 1990)

We have studied the Shubnikov-de Haas oscillations in *n*-type gray tin films in which several size-effect-quantized subbands are relevant. The observed oscillations at oblique magnetic-field angles become increasingly two dimensional in character as the film thickness decreases. In addition, frequencies associated with nonextremal cross sections of the Fermi surface are observed.

PACS numbers: 71.25.Hc, 72.15.Gd

A thin film with a thickness comparable to the effective carrier de Broglie wavelength can have a size-effect-quantized energy spectrum. In the limit of one bound state in the direction perpendicular to the film, phenomena such as the Shubnikov-de Haas (SdH) oscillations and the quantum Hall effect have been widely studied (e.g., silicon inversion layers or single-level quantum wells in modulation-doped AlAs/GaAs heterostructures).<sup>1,2</sup> Less is known about the intermediate region where several size-quantized subbands are relevant and the quantum transport coefficients involve two incommensurate length scales: the cyclotron diameter  $D$  and the film thickness  $d$ .

Gray tin films grown by molecular-beam epitaxy (MBE) provide a unique medium to study the quantum transport phenomena in this intermediate region due to their relatively high carrier mobility and smooth surfaces. More importantly, *n*-type gray tin, unlike bismuth films or whiskers, where three tilted electron ellipsoids and one hole ellipsoid are involved,<sup>3</sup> has but a single spherical sheet of the Fermi surface, which facilitates distinguishing different effects. In this Letter we report systematic studies of the SdH oscillations in MBE-grown gray tin films in the size-effect-quantized regime as a function of the thickness, temperature, and magnetic field (both magnitude and direction). The observed oscillations manifest electronic subbands, which become increasingly two-dimensional in character as the film thickness is reduced.

The gray tin films were grown epitaxially on (001) CdTe wafers with a custom-designed MBE system.<sup>4</sup> The oscillatory magnetoresistance and Hall coefficient were measured using the field-modulation technique in a variable-temperature cryostat capable of temperature down to 1.2 K and fields up to 12 T. Data acquisition was controlled by a computer. The data to be discussed here were taken on *n*-type gray tin films measuring  $5 \times 5$  mm<sup>2</sup> with nominal thicknesses of 800 (sample *A*), 1000 (sample *B*), and 1600 Å (sample *C*), which were determined from the calibrated growth rate. All three samples were prepared consecutively in the MBE apparatus (without cycling to atmospheric pressure). The temperature dependence of the resistance at zero field exhibits a large resistance peak at  $\sim 140$  K; this peak arises from a

crossover of the dominant conduction electron carriers from the three [111]  $L$ -centered valleys at room temperature to a single  $\Gamma$ -centered band minimum at low temperatures.<sup>4,5</sup> The carrier concentration in the  $T=0$  limit was  $\sim (2.5-2.7) \times 10^{17}$  cm<sup>3</sup> and the Hall mobility  $\mu_H$  was  $\sim 8000$  cm<sup>2</sup>/V sec for all three specimens. The van der Pauw four-contact geometry<sup>6</sup> that was employed is shown schematically as the inset of Fig. 1(b), where  $\mathbf{n}$  denotes the film plane normal. For each contact configuration (see Ref. 6), measurements were carried out at different temperatures between 2 and 8 K and for three field orientations: 0°, 45°, and 90° (with respect to the film plane normal).

Figure 1(a) shows a recording of the oscillatory magnetoresistance for an 800-Å-thick film obtained by detecting the first harmonic of the modulation frequency. The magnetic field is perpendicular to the film surface. A beat structure is evident which will be discussed in detail below. One of the key tests of 2D character is the behavior of the oscillations as the field is tilted away from the plane normal. A strictly 2D system will have oscillatory properties which only involve the normal component of the field.<sup>1</sup> Shown in Fig. 1(b) is the oscillatory Hall resistivity for sample *A* measured at 2.1 K with  $\mathbf{H}$  at 45° to  $\mathbf{n}$ . A beat structure is clearly seen. The arrow in this figure indicates the classical size-effect-cutoff field  $H_{\text{cut}}$  defined by  $D = 2c\hbar k_F/eH = \sqrt{2}d$ , where  $D$  is the cyclotron orbit diameter,  $k_F$  is the Fermi wave number, and  $\sqrt{2}d$  is the projected film thickness. Clear oscillations set in at fields much lower than  $H_{\text{cut}}$ . The magnetoresistance of this sample shows essentially the same oscillatory behavior. The oscillatory amplitudes below  $H_{\text{cut}}$  for the 45° case depend strongly on the film thickness: Qualitatively, the observed amplitudes for the 1000-Å-thick sample are smaller than those for 800 Å, and for the 1600-Å-thick sample the oscillations are barely detectable.

The energy spectrum of bulk electrons in a parabolic band with the magnetic field  $\mathbf{H}$  in the  $z$  direction is

$$E = (n + \frac{1}{2})\hbar\omega_c + \hbar^2 k_z^2 / 2m_z^* \pm \frac{1}{2}g\mu_B H, \quad (1)$$

where  $\omega_c = eH/m^*c$ ,  $m^*$  is the effective cyclotron mass,  $\mu_B$  is the Bohr magneton, and  $g$  is the effective spin-splitting factor. The constant-energy surfaces in  $\mathbf{k}$  space

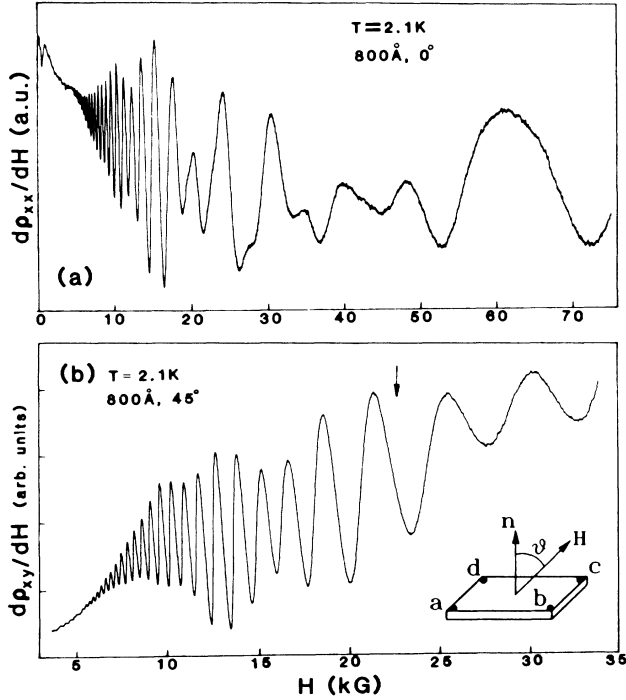


FIG. 1. (a) SdH oscillations for sample *A* at 2.1 K vs magnetic field *H* with **H** parallel to the film plane normal. (b) The first derivative  $d\rho_{xy}/dH$  vs magnetic field for sample *A* at 2.1 K with the field tilted  $45^\circ$  from the film plane normal. The arrow indicates the corresponding cutoff field. Inset: van der Pauw contact geometry. [Note that curves in (a) and (b) are  $180^\circ$  out of phase.]

perpendicular to the field become quantized according to the Onsager relation:  $(2\pi eH/\hbar c)(n + \gamma) = A_n$ , where  $A_n$  is the cross-sectional area corresponding to quantum number  $n$  and  $\gamma$  is a phase factor ( $\frac{1}{2}$  in the present case). The period of the oscillation is given by

$$P = \Delta(1/H) = 1/F = 2\pi e/c\hbar A_e, \quad (2)$$

where  $A_e$  is the extremal cross-sectional area of the Fermi surface perpendicular to the field and  $F$  is the oscillation frequency. In Fig. 2 we have plotted the values of  $1/H$  at which maxima occur in the oscillations versus the quantum number  $n$  for both the  $0^\circ$  and  $45^\circ$  cases. The periods (as determined by the slopes) are listed in Table I. The salient feature of the data is that it reveals a gradual 3D-2D transition as the film thickness is reduced. As shown in Table I, the ratios  $P(45^\circ)/P(0^\circ)$  are 1.0, 0.82, and 0.74 for samples *C*, *B*, and *A*, respectively. In the extreme case of a 2D band, the oscillations should depend only on the *normal component* of the field, i.e.,  $H \cos\theta$ , and one expects  $P(45^\circ)/P(0^\circ) \approx 0.707$ . Clearly, the behavior of sample *A* is essentially two dimensional (or quasi-2D) in character.

The above picture is further supported by examining the temperature and field dependence of the amplitudes.

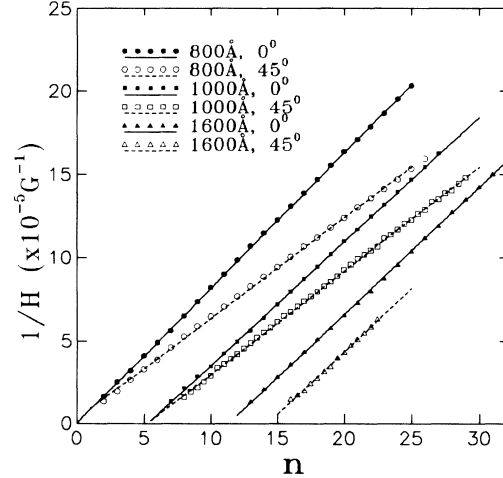


FIG. 2. Nodal positions of the SdH oscillations vs quantum number  $n$  for samples *A*, *B*, and *C*.

The amplitude of the first harmonic in the Adams-Holstein expression<sup>7</sup> is given by

$$A_1 \propto \frac{T \exp(-\beta T_D m'/H)}{H^{1/2} \sinh(\beta T m'/H)}, \quad (3)$$

where  $m' = m^*/m_e$  is the reduced mass,  $\beta = 2\pi^2 k_B m_e c / e\hbar = 14.692$  T/K,  $m_e$  is the electron mass, and  $T_D$  is the Dingle temperature. Note that a two-dimensional system has the same temperature dependence but with a different prefactor.<sup>2</sup> For a tilted 2D system, the normal component,  $H \cos\theta$ , enters the above expression; equivalently, we can say that the reduced mass is "enhanced" by a factor of  $1/\cos\theta$ . Figure 3(a) shows the fit by Eq. (3) for the amplitude of the oscillatory magnetoresistance of sample *A* at 1 T. The reduced masses are 0.046 and 0.032 for the  $45^\circ$  and  $0^\circ$  cases, respectively. Their ratio is very close to  $1/\cos 45^\circ$ . At sufficient low fields, the sinh term in Eq. (3) can be replaced by its exponential form. Including the Bessel-function factor associated with the field-modulation technique,<sup>8</sup> the amplitude at a fixed temperature depends on the field as

$$dA_1/dH \propto (T/H^{5/2}) \exp[-\beta(T + T_D)m'/H].$$

Figure 3(b) shows  $\ln(AH^{5/2})$  vs  $1/H$  plots for sample *A*.

TABLE I. Oscillation periods and frequencies for samples, *A*, *B*, and *C*.  $N_e$  is the quantum number corresponding to the Fermi level.

Sample	<i>d</i> (Å)	<i>P</i> ( $10^{-2}$ T $^{-1}$ )		<i>F</i> <sub>0</sub> (T)		<i>F</i> ' (T)		<i>N</i> <sub><i>e</i></sub>
		0°	45°	0°	45°	0°	45°	
<i>A</i>	800	8.1	6.04	12.7	16.9	9.15	13.02	4-5
<i>B</i>	1000	7.6	6.24	13.1	16.5	10.3	12.77	6
<i>C</i>	1600	7.6	7.6	13.0	13.3	11.5	...	9-10

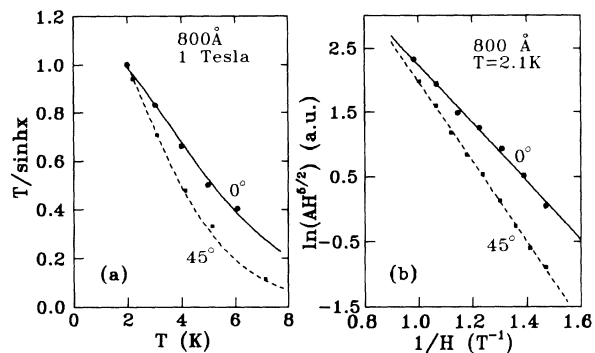


FIG. 3. (a) The temperature dependence of the SdH amplitudes of sample *A* at 1 T for the  $0^\circ$  and  $45^\circ$  cases. The solid curves are a fit by Eq. (3), and  $x \equiv \beta m^* T/H$  as described in the text. (b) Plots of  $\ln(AH^{5/2})$  vs  $1/H$  for sample *A* at 2.1 K.

The resulting slopes are  $-4.517$  and  $-6.183$  for the  $0^\circ$  and  $45^\circ$  cases, respectively. The ratio of the slopes is 0.73, again consistent with a nearly 2D-like behavior for sample *A*. A similar analysis based on oscillatory amplitudes of the Hall resistance yields essentially the same results. Using the reduced mass  $m^* \sim 0.032$ , the calculated Dingle temperature is  $T_D \sim 7.4$  K.

To explore the origin of the beat structure observable in Fig. 1, a spectrum analysis was performed by using the fast-Fourier-transform (FFT) technique. Typical FFT spectrums are shown in Fig. 4 for sample *A* at two field orientations. Evidently, the oscillations are dominated by a fundamental frequency  $F_0$  ( $F_0 = 12.7$  T for the  $0^\circ$  case). The error in the frequency determination is  $\pm 0.3$  T. The second harmonic yields only a small contribution, which justifies the first-harmonic approximation adopted above. The peak at zero frequency stems from the monotonically increasing static magnetoresistance. Also resolved is a small peak at a frequency  $F'$  which is responsible for the observed beat structure. The values of the frequencies  $F_0$  and  $F'$  for the three samples and the different field orientations are listed in Table I. Note that the ratios  $F_0(0^\circ)/F_0(45^\circ)$  are consistent with a dimensional-crossover behavior. The smaller frequencies  $F'$  in the spectrum cannot be attributed to spin splitting<sup>1</sup> since  $\Delta F \equiv F_0 - F'$  increases with decreasing film thickness (see Table I). Even though an effective  $g$  factor as large as 28 has been reported for gray tin single crystals,<sup>9</sup> it is not expected that a reduction in film thickness will modify the spin-orbit coupling (which leads to the  $g$  shift) to such an extent; furthermore, the spin splitting is governed by the *total magnetic field* and is thus *independent* of the field direction.<sup>1,2</sup> In contrast, the data in Table I show that for sample *A*,  $F'(\theta)$  scales roughly as  $\cos\theta$ . A reasonable interpretation is that the appearance of  $F'$  is a manifestation of the quantum size effect. In the presence of quantization along the film normal, the Fermi surface is replaced by a set of disks with  $k_z$  values given by  $k_z = \pi N/d$ ; here  $N$  is

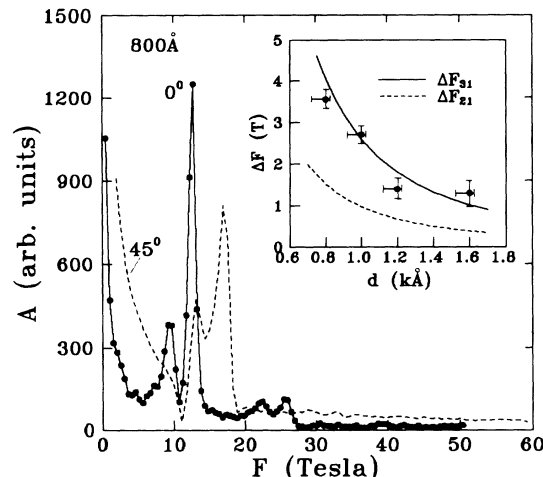


FIG. 4. The FFT spectrum of sample *A* for two field orientations. Inset: Plot of the frequency difference vs  $d$ . The experimental values of  $\Delta F (=F_0 - F')$  are shown as circles; the dashed and solid lines show the calculated frequency reduction associated with the  $N=1$  and the  $N=2$  and  $N=3$  levels, respectively.

a quantum number. The oscillation period associated with the  $N$ th allowed cross section is  $P_N = 2\pi e/\hbar c A(E_F, N)$ .<sup>10</sup> As a result SdH oscillations from each size-effect subband should be present at some level. Experimentally not all of them may be observable due to (i) a very close spacing (the  $N=1$  and 2 levels) or (ii) a shorter scattering time (for levels with higher  $N$  values). The plot of the frequency difference between  $F_0$  and  $F'$  versus  $d$  is shown in the inset of Fig. 4. In this inset the dashed and solid lines are the calculated frequency reductions corresponding to the  $N=1$  and the  $N=2,3$  levels, respectively. Even though interdiffusion tends to reduce the effective film thickness, our measured beat frequency is close to that expected for an interference between the  $N=1$  and  $N=3$  levels.

The size effect is most prominent when the magnetic field lies in the film plane. For this case, even the dc magnetoresistance exhibits oscillations with large amplitudes. For  $H > H_{\text{cut}}$ , the period is identical to that for the  $0^\circ$  case; for  $H < H_{\text{cut}}$ , the periods increase with decreasing magnetic field which may be associated with skipping orbits involving specular reflection off the film surfaces.

In summary, we have studied the SdH oscillations in gray tin films in the size-quantization regime. The observed transition from 3D to 2D behavior for the  $45^\circ$  case may be due to the fact that the number of final states, associated with different values of (an appropriately generalized quantum number)  $N$ , decreases with  $d$ . Whatever the explanation, our experiments demonstrate that the transition from 3D- to 2D-like behavior in the Shubnikov-de Haas effect as a film is thinned is *not* abrupt. The subbands of an 800-Å-thick film display an

essentially two-dimensional behavior.

This work was supported by the Materials Research Center under Grant No. DMR 85-20280 and the NSF division of Low Temperature Physics under Grant No. DMR 89-07396.

---

<sup>1</sup>F. F. Fang and P. J. Stiles, *Phys. Rev.* **174**, 823 (1968); M. Kobayashi and K. F. Komatsubara, *Solid State Commun.* **13**, 293 (1973).

<sup>2</sup>For a review, see T. Ando, A. B. Fowler, and F. Stern, *Rev. Mod. Phys.* **54**, 437 (1982); L. L. Chang, H. Sakaki, C.A. Chang, and L. Esaki, *Phys. Rev. Lett.* **38**, 1489 (1977).

<sup>3</sup>N. B. Brandt, D. B. Gitsu, V. A. Dolma, and Y. G. Ponomarev, *Zh. Eksp. Teor. Fiz.* **92**, 913 (1987) [*Sov. Phys. JETP* **65**, 515 (1987)]; *Fiz. Nizk. Temp.* **13**, 193 (1987) [*Sov. J. Low Temp. Phys.* **13**, 107 (1987)].

<sup>4</sup>L. W. Tu, G. K. Wong, and J. B. Ketterson, *Appl. Phys. Lett.* **54**, 1010 (1989).

<sup>5</sup>O. N. Tufte and A. W. Ewald, *Phys. Rev.* **122**, 1431 (1961).

<sup>6</sup>L. J. van der Pauw, *Philips. Res. Rep.* **13**, 1 (1958). Three contact configurations were used. For configuration 1, the current leads are *a* and *b*, and the potential leads are *d* and *c*. For configuration 2 (3), the current leads are *a* and *d* (*c*). To determine  $\mu_H$ , both the current and field directions were reversed as required. As a result of the (001) epitaxy of the film, the geometry factor in van der Pauw's resistivity expression is approximately unity. The data presented in Figs. 2-4 were all obtained using configuration 1.

<sup>7</sup>E. N. Adams and T. D. Holstein, *J. Phys. Chem. Solids* **10**, 254 (1959).

<sup>8</sup>A. Goldstein, S. J. Williamson, and S. Foner, *Rev. Sci. Instrum.* **36**, 1356 (1965); L. R. Windmiller and J. B. Ketterson, *ibid.* **39**, 1672 (1968).

<sup>9</sup>B. L. Booth and A. W. Ewald, *Phys. Rev. Lett.* **18**, 491 (1967).

<sup>10</sup>V. N. Jutskii and T. N. Pinsker, *Thin Solid Films* **66**, 55 (1980).